Mechanical and Morphological Study of Polyphenylene Sulfide/Liquid Crystalline Polymer Blends Compatibilized with a Maleic Anhydride Grafted Copolymer

T. Rath,[1] S. Kumar,[1] R. N. Mahaling,[1] C. K. Das,[1] S. B. Yadaw[2]

[1]*Materials Science Centre, Indian Institute of Technology, Kharagpur 721302, India*
[2]*Defence Materials and Stores Research Development and Establishment, Kanpur 280013, India*

Received 27 October 2006; accepted 3 June 2007
DOI 10.1002/app.27047
Published online 30 August 2007 in Wiley InterScience (www.interscience.wiley.com).

ABSTRACT: Blends of thermotropic liquid crystalline polymer (LCPA-950), based on a copolyester of hydroxynapthoic acid and hydroxybenzoic acid with an engineering thermoplastic, poly(phenylene sulfide) (PPS), were prepared using a corotating twin-screw extruder. Addition of a third component, a functionalized polypropylene (maleic anhydride grafted polypropylene, MA-PP), that interact with the thermotropic liquid crystalline polymer (TLCP) facilitates the structural development of the TLCP phase by acting as a compatibilizer at the interface. Differential scanning calorimetry and dynamic mechanical thermal analysis results, however, show that there is an interaction between the polymers in the presence of compatibilizer. This means that MA-PP can be used as a compatibilizer for the PPS/LCP *in situ* composite system. The viscosity of the compatibilized *in situ* composite was decreased by the compatibilizer, and this is mainly due to the fibrous structure of the LCP at the high shear rate. The mechanical properties of the ternary blends were increased when a proper amount of MA-PP was added. This is attributed to fine fibril generation induced by the addition of MA-PP. Morphological observations determined the significance of the third component in immiscible polymer blends, and an optimum amount of MA-PP exists for the best mechanical performance. © 2007 Wiley Periodicals, Inc. J Appl Polym Sci 106: 3721–3728, 2007

Key words: compatibilization; liquid crystalline polymer; graft copolymer; mechanical properties and morphology

INTRODUCTION

A frequent goal of polymeric material research is the improvement of physical properties. An approach that is widely used is the combination of two polymers in the hope of obtaining favorable properties in the blend. If successful, this route can lead to the creation of attractive new composite materials. One relatively new type of blend is that of thermotropic liquid crystalline polymers (TLCPs) and thermoplastics (TP) matrices, the high modulus of LCP can form *in situ* fibrils, which reinforce the TP matrix because there is high molecular orientation in the fibrils. The LCP can also serve as processing aids in extrusion and injection molding because of their low melt viscosity. These materials display *in situ* self-reinforcing properties and the termed molecular or microfibrillated composites.[1–4] These properties make blends of LCPs and TPs ideal candidates for high-performance engineering applications. The morphology of the LCP domains dominates many of the final physical properties of the blend. The issues controlling the morphology and ultimate physical properties of a LCP/polymer blend are quite complex. The rheological behavior of blend components, interfacial tension, and processing conditions are known to be the key factors governing the morphology. To obtain good fibrillation, high loading of LCP is usually used so as to reach a critical LCP content. This generally makes the materials impractical economically, and so the advantages of LCP in polymer blends have yet to be fully exploited.[5] Although great efforts have been made to modify the property and processability of *in situ* composites, the main problems associated with the blends of LCP/TPs, e.g., poor adhesion of interfaces between LCP and polymer matrix, and difficulty in controlling processing parameters for LCP fibrillation, remains unsolved.[6]

A primary question in the studies of blends of LCPs and TPs is the role of the interfacial properties in the formation of a fibrous minor phase. Most of the TP polymers studied so far are incompatible with commercially available LCPs.[7] Wholly aromatic TLCP, such as vectra LCP, a copolyester consist of 4-hydroxybenzoic acid (HBA) and 2-hydroxy-6-naphthoic acid (HNA), have been shown to display no

Correspondence to: C. K. Das (chapal12@yahoo.co.in).

Journal of Applied Polymer Science, Vol. 106, 3721–3728 (2007)

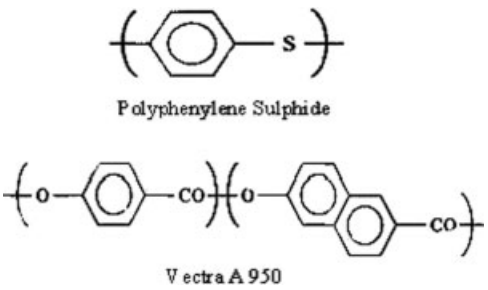

Figure 1 The structure of PPS and LCP.

miscibility and poor compatibility poly(phenylene sulfide) (PPS).[8–10] According to Tsebrenko and Danilova, the immiscibility or poor compatibility between a LCP and its polymer matrix is one of the basic conditions for flow-induced fiber formation.[11] However, poor interfacial adhesion between the components in these multiphase mixtures is often responsible for the poor mechanical properties such as tensile strength and fractured toughness.

To promote interfacial adhesion between TPs and LCP components, researches have attempted various techniques such as long flexible spacers[12]; block copolymers[13]; functional groups with similar chemical structure to the compounded polymers[14]; and addition of third reactive component.[15] When applying any techniques to two phases by either reactive or nonreactive agents, however, the reactivity must be carefully controlled, because while the compatibilizer improves interfacial adhesion, it may also prevent *in situ* fiber formation. An uncontrolled compatibilization between the dispersed phase and its matrix may reduce the numbers and the lengths of the *in situ*-formed LCP fibers or even convert the fibers into droplet domains.[16]

In this work, the morphology, miscibility, and mechanical property relationships of PPS/LCP blends were examined. The compatibilizing effects of maleic anhydride grafted polypropylene (MA-PP) on the mechanical property and the LCP fibrillation of the blends will also be discussed.

MATERIALS

The TLCP used in this study was Vectra A950 supplied by Ticona (Shelby, NC). This LCP is a wholly aromatic copolyester consisting of 25 mol % of 2,6-hydroxynaphthoic acid (HNA) and 75 mol % of *p*-hydroxybenzoic acid (HBA). The molecular weight could not be determined because it was difficult to find a suitable solvent in which it can be dissolved. The thermoplastic used in this study was poly(phenylene sulfide), grade Fortron 0214C1, which was obtained as a pellet from DMSRDE (Kanpur, India). The molecular weight was determined in chloronapthalene by gel permeation chromatography at 215°C. The results were M_w = 42,012, M_n = 5762, and M_z = 82,466 with polydispersities of 7.29 (M_w/M_n) and 1.96 (M_z/M_w). Maleic anhydride grafted polypropylene copolymer (MA-PP) with 0.6 wt % maleic anhydride content was supplied by Aldrich Chemicals and used as a compatibilizer. The structures of PPS and LCP are given in Figure 1.

EXPERIMENTAL

Blending and extrusion

The pellets of the PPS and Vectra-A950 were dried in a vacuum oven at 70°C for 24 h before use. MA-PP was dried in a vacuum oven at 80°C for 24 h. Dried pellets of liquid crystalline polymer and PPS, and MA-PP were mixed in a container before blending the extruder. Blending was carried out using a Brabender Plasti-Corder PL 2200 (mixer N50) twin-screw extruder at a fixed rotation speed of 30 rpm. The screw had a diameter of 19 mm, L/D of 25. The extrusion temperature of the feeding zone/transporting zone/melting zone/die were set as 160/300/300/290°C, respectively. Blending formulation is given in Table I.

Thermal properties

Differential scanning calorimetry (DSC) measurements of the thermal property characteristics were performed on a NETZSCH DSC 200PC. The samples (6.5 mg) sealed under aluminum pans were scanned in the temperature range of room temperature to 650°C at a heating rate of 10°C/min and was allowed to crystallize at a cooling rate of 10°C/min under the nitrogen atmosphere with a flow rate of 40 mg/min. Dynamic mechanical thermal analysis (DMTA) of the blends were conducted with a DMTA-2980 (TA Instruments). A single cantilever clamp was used, and a frequency of 1 Hz and an amplitude of 15 μm was applied on the samples. The temperature range was 50–250°C at a heating rate of 5°C/min. The storage modulus (E') and tan δ were measured for each sample in this temperature range.

Rheology

Rheology measurements were carried out on an Instron capillary rheometer Model. Samples were loaded

TABLE I
Compounding Formulation

Sample no.	M1	M2	M3	M4
PPS	100	75	75	75
LCP-A	–	25	25	25
MA-PP	–	–	2	5

All the contents are in phr.

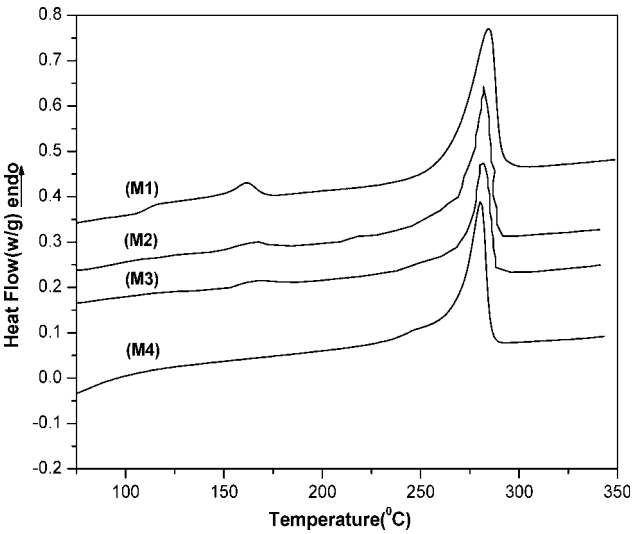

Figure 2 DSC thermograms of melting behavior of PPS and the blends: (M1) PPS, (M2) binary blend, (M3) 2% MA-PP-added ternary blend, and (M4) 5% MA-PP-added ternary blend.

in pellet from at 300°C. Approximately 15 min was required following loading for the system to reach thermal equilibrium. Capillary of diameter 0.762 mm (L/D = 33.3) was employed to cover a shear rate of 50×10^2 to 4×10^2 s^{-1}.

X-ray diffraction

X-ray diffraction (XRD) was performed with a PW 1840 X-ray diffractometer using copper target (Cu Kα) at a scanning rate of 0.05°2θ/s between 10° and 60°, accumulation time 25 s, chart speed of 10 mm/2θ, range of 5000 c/s, and a slit of 0.2 mm, operating at a voltage of 40 kV and current of 20 mA to assess the change of crystallinity of the blends as a function of blend ratio.[17]

Scanning electron microscopy study

The morphology of the fractured surfaces of the blends was observed using a Jeol JSM-scanning electron microscope (SEM). To observe the dispersion and distribution of LCP particles, tensile bars were crayofractured in liquid nitrogen. The fractured surfaces were gold plated and then mounted over aluminum stub using a double-sided electric adhesive tape. The vacuum was in the order of 10^{-4}–10^{-6} mmHg during scanning of the composite samples.

Mechanical properties

To measure the mechanical properties of the blends, tensile testing was repeated for at least four samples at an extension speed of 10 mm/min, with an initial gauge length of 35 mm and a width of 4.5 mm using a universal tensile testing machine, a Hounsfield HS 10 KS, at room temperature.

RESULTS AND DISCUSSION

Thermal properties

The results from the DSC scans for the binary and ternary blends are presented in Figure 2. The thermal properties of the blends are summarized in Table II. The glass transition temperature, T_g, was evaluated by DSC and then related to the DMTA point at which tan δ is a maximum. Before the analysis of the ternary blends, binary blends of PPS and LCPA were studied. The T_g of PPS is known to be 106°C and that of LCPA to be 104°C. The melting endotherm of LCPA is not apparent because of its small heat of fusion. It is not clear from the DSC thermograms whether the LCPA phase forms its own domains or is mixed in the PPS. The binary blends display multiple peaks. This phenomenon can be explained by the existence of different kinds of crystallization processes.[18] A more perfect crystal population has a higher melting temperature at the main peak. The smaller secondary crystals are less perfect and melt to form the secondary peaks. The appearance of multiple melting peaks implies that mixing with LCPA affects the crystallization process of PPS. The recrystallization peaks which appear upon cooling the various blends are shown in Figure 3. In each case, the samples were held at 300°C for 2 min after heating and then cooled at a rate of 10°C/min. The pure PPS shows a crystallization-point maximum of about 231°C. But this crystallization point shifts to the lower temperature side with the addition of LCPA. It appears from the melting and the crystallization data that the TLCP phase acts as a nucleating agent. Though TLCP phase affects the crystallization rate of PPS, it does not seem to change the crystallization structure as seen from the X-ray spectra. The maximum of tan δ from DMTA is shown in Figure 4. The T_g of PPS is 112°C and the peak at 100°C is assigned to that of VA. The T_g values obtained from dynamic mechanical analysis are higher than those obtained from thermal analysis. Such a difference is reasonable when one takes the features of these measuring techniques into consideration. The appearance of separate T_gs indicates that PPS and LCPA are immiscible.

TABLE II
Thermal Properties of the Blends

Sample	T_m (°C)	T_c (°C)	ΔH (J/g)
M1	284	231	27.5
M2	282	228	23.4
M3	281	224	21.2
M4	280	218	18.7

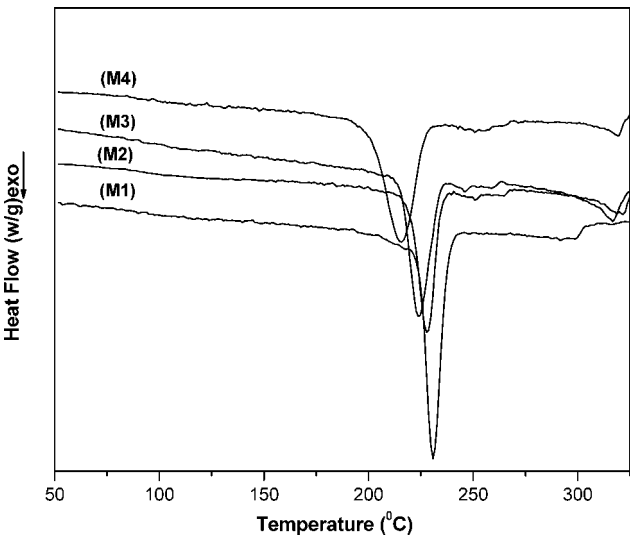

Figure 3 DSC thermograms of cooling process for PPS and blends: (M1) PPS, (M2) binary blend, (M3) 2% MA-PP-added ternary blend, and (M4) 5% MA-PP-added ternary blend.

In the ternary blends, the appearance of minor melting peaks in addition to the major melting transition of PPS around 282°C indicates that addition of MA-PP also affects the crystallization process of PPS (Fig. 2). The melting temperature (T_m) of PPS does not show a remarkable variation with MA-PP addition. The crystallization–peak temperature shifts to a lower temperature with the addition of MA-PP (Fig. 3). This is ascribed to the added MA-PP reacting with VA and PPS to produce a compatibilizer that makes the blend more homogeneous.[19,20] This supports the conclusion that LCPA, the added MA-PP, or both are acting as a nucleating agent. Changes in the crystallization process are believed to occur because of altered nucleation and growth conditions in the ternary blends. Excess MA-PP may form a separate phase, which can act as an impurity in the blend.

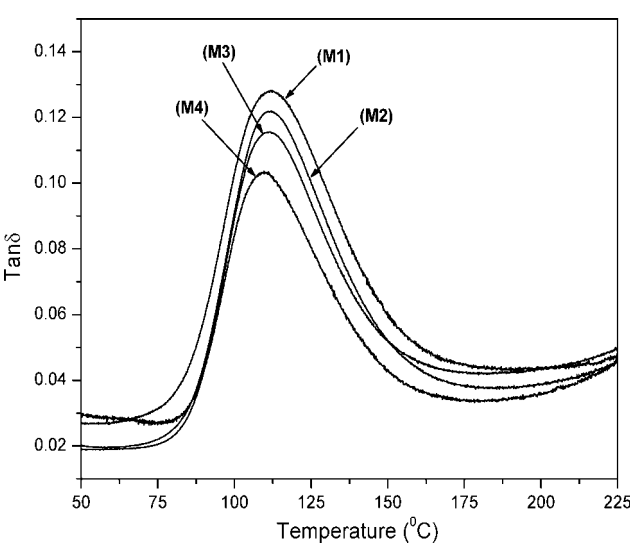

Figure 4 Normalized tan δ versus temperature for binary and ternary blends: (M1) PPS, (M2) binary blend, (M3) 2% MA-PP-added ternary blend, and (M4) 5% MA-PP-added ternary blend.

Rheological properties

The flow curves of the pure components and ternary blend measured at 300°C are depicted in Figure 5. It can be seen from the figure that, in the shear rate range studied, all the melts exhibit a typical non-Newtonian behavior. The semirigid LCP sample shows a viscosity lower than that of the PPS. The processing shear rate (apparent shear rate) was about 4×10^2 s^{-1}, and PPS has a viscosity nearly one order of magnitude higher that that of LCP. The viscosity of the blend in the investigated shear-rate range was intermediate between the two neat polymers. Evidently polymer chains in LCP try to become more and more oriented in the melt by shearing forces, which makes it easier to slide past one another thus reducing the viscosity. Ternary blends show viscosities even lower than those of binary blends. The reduction in viscosity of the blends can possibly be attributed to interfacial slippage between the two polymers.[21] Since the PPS-LCP blends are incompatible, the LCP domains in the melt state having low viscosity possibly migrate toward the capillary surface and act as a lubricating layer over the capillary surface. This results in a reduced blend viscosity.

Figure 6 shows the variation of storage modulus (E') as a function of temperature for the blends and the pure PPS. The pure PPS exhibits a sharp

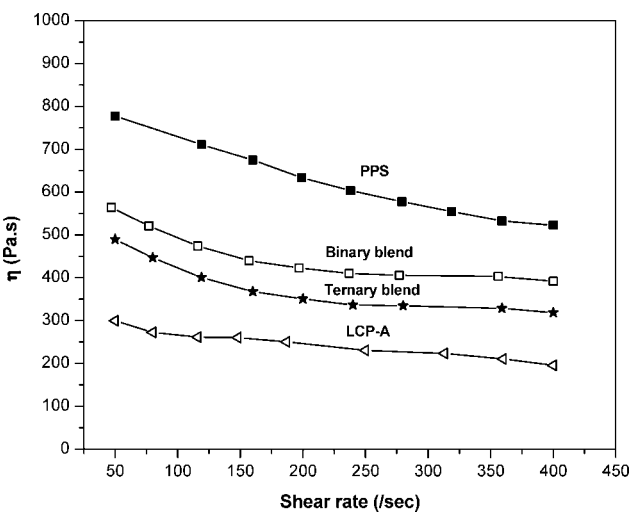

Figure 5 Viscosity–shear rate relationship at 300°C (■) PPS, (□) binary blend, (★) 2% MA-PP-added ternary blend, (◁) LCP-A

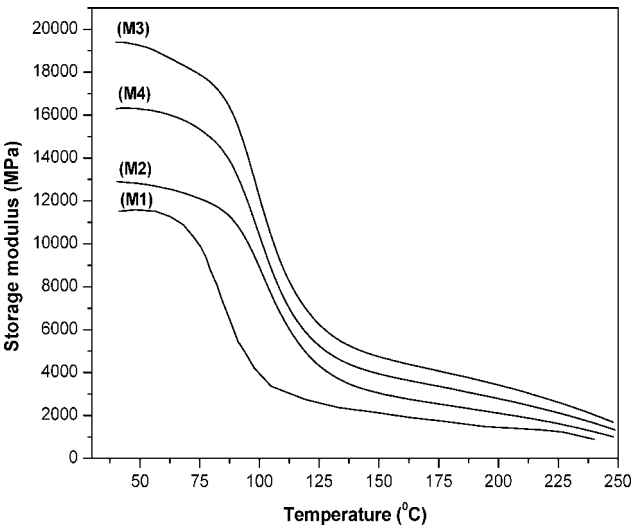

Figure 6 DMTA measurements of storage modulus (E'). (M1) PPS, (M2) binary blend, (M3) 2% MA-PP-added ternary blend, and (M4) 5% MA-PP-added ternary blend.

decrease in the value of the storage modulus at the glass transition region corresponding to the temperature range of 70–100°C. This is followed by a plateau, which extends to a temperature of 250°C. Addition of LCP to PPS was found to increase the storage modulus value. Above the T_g of pure PPS the E' value increases with the addition of LCP content and also the modulus in the plateau was found to increase. This increase in the modulus of the plateau is beneficial as this ensures better performance of blends at high temperature. We also estimated an increase in storage modulus above T_g, suggesting that the crystallization of PPS under the dynamic strain conditions is due to the nucleation and interaction between the LCP and the matrix. It is also evident that even at higher temperatures the blend storage modulus was higher than the storage modulus of pure polymer at lower temperatures. This validates the point that the LCP is an effective reinforcing agent for PPS even at higher temperature. But this increase is prominent in the presence of compatibilizer and the improvements are observed for the entire temperature range scanned. This implied that the addition of MA-PP has lead to an improvement in the compatibility between the blend components. However, E' in the plateau region (below the T_g) is higher for the MA-PP concentration of 2%, which is consistent with the static tensile data.

XRD- measurement

The XRD experiment was performed on samples of the PPS and PPS/LCP blends in the presence and absence of compatibilizer, and the diffractograms are shown in Figure 7. From Figure 7 it was observed that the diffraction pattern of the PPS and PPS/LCP blend appears to be similar; whereas a slight decrease in intensity was observed for the PPS/LCP blend. The blends with LCP show a decrease in intensity at about $2\theta = 20^\circ$, while other peaks corresponding to the PPS remain unchanged in their peak position and intensities. Addition of compatibilizer to the PPS/LCP blends, the crystalline peak of PPS at $2\theta = 20^\circ$ showing a significant decrease in the peak intensity, indicates that the compatibilizer affects the ordered structure of PPS by reacting at the interface between LCP and PPS by forming graft copolymers. The percentage of crystallinity of the blends is decreased by the addition of LCP (Table III). However, this decrease is prominent in the presence of compatibilizer. In the presence of compatibilizer the PPS/LCP blend shows lower crystallinity than all other systems. This suggests that the reactivity of the compatibilizer toward LCP and PPS is more efficient. As it was known that the compatibilized blends show always lower crystallinity than those of the uncompatibilized blends due to the random structure of the formed graft/block copolymers, which will modify the ordered structure of base polymers. Hence, the crystallinity of the blends decreases by the addition of compatibilizers.

Morphologies of the blends

In an effort to provide more support for the compatibility of the ternary blend, the morphologies of binary (PPS/LCPA) and ternary (PPS/LCPA/MA-PP) blends were investigated. SEM micrographs of the fractured surfaces of binary blends are shown in

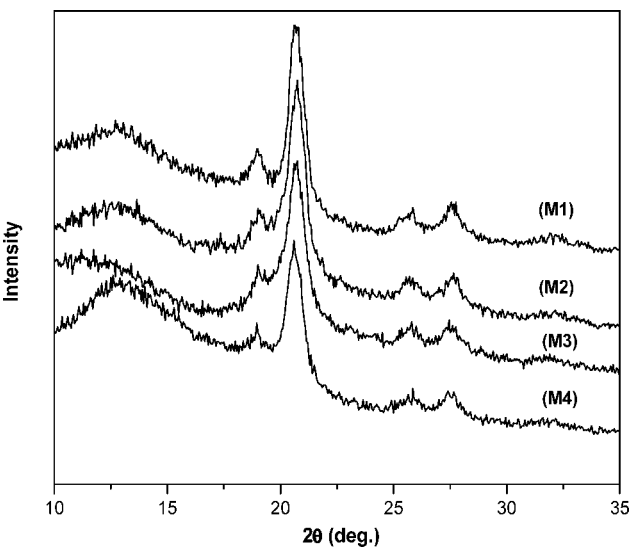

Figure 7 XRD spectra of PPS, binary blend and ternary blends. (M1) PPS, (M2) binary blend, (M3) 2% MA-PP-added ternary blend, and (M4) 5% MA-PP-added ternary blend.

TABLE III
Percentage Crystallinity of the Blends

Mix. no.	Crystallinity (%)
M1	54
M2	47
M3	37
M4	33

Figure 8. In the binary blend Figure 8M1, void formation resulting from phase separation, a dispersed spherical phase, and poor adhesion between the TLCP and the matrix are observed. The mechanical properties of the binary blend are poor as a result of this morphology. In the binary blend of PPS/LCPA, the TLCP domains are relatively large because of immiscibility, thereby leading to poor dispersion. The micrographs also demonstrate poor adhesion between the two phases, which leads to an open ring hole around the TLCP domain while TLCP is pulled out during the fracture of the samples. The ternary blend surface Figure 8M3 and 8M4 shows a different morphology. The size of the dispersed phase is noticeably reduced. The fractures are seen to occur within the strands in the ternary blend when 2% MA-PP is added. There is no open ring hole around the TLCP domain, reflecting better adhesion between the two phases. Furthermore, the VA phase shows fibril shapes that are uniformly distributed and which are finer than those in the LCPA phase of the binary blends (Fig. 8M2). When 5% MA-PP is added, a complicated morphology appears (Fig. 8M4). Fine TLCP fibril shapes are still observable, but some have been incorporated into large domains. Excess levels of MA-PP seem to induce coagulation or flocculation of the dispersed TLCP phase.

Mechanical properties

The morphological differences between blends with and without MA-PP definitely affect their respective physical properties. The tensile strength and tensile modulus of the binary and ternary blends are shown in Figure 9(a,b). It can be seen in this figure that binary blend shows a negative deviation from the rule

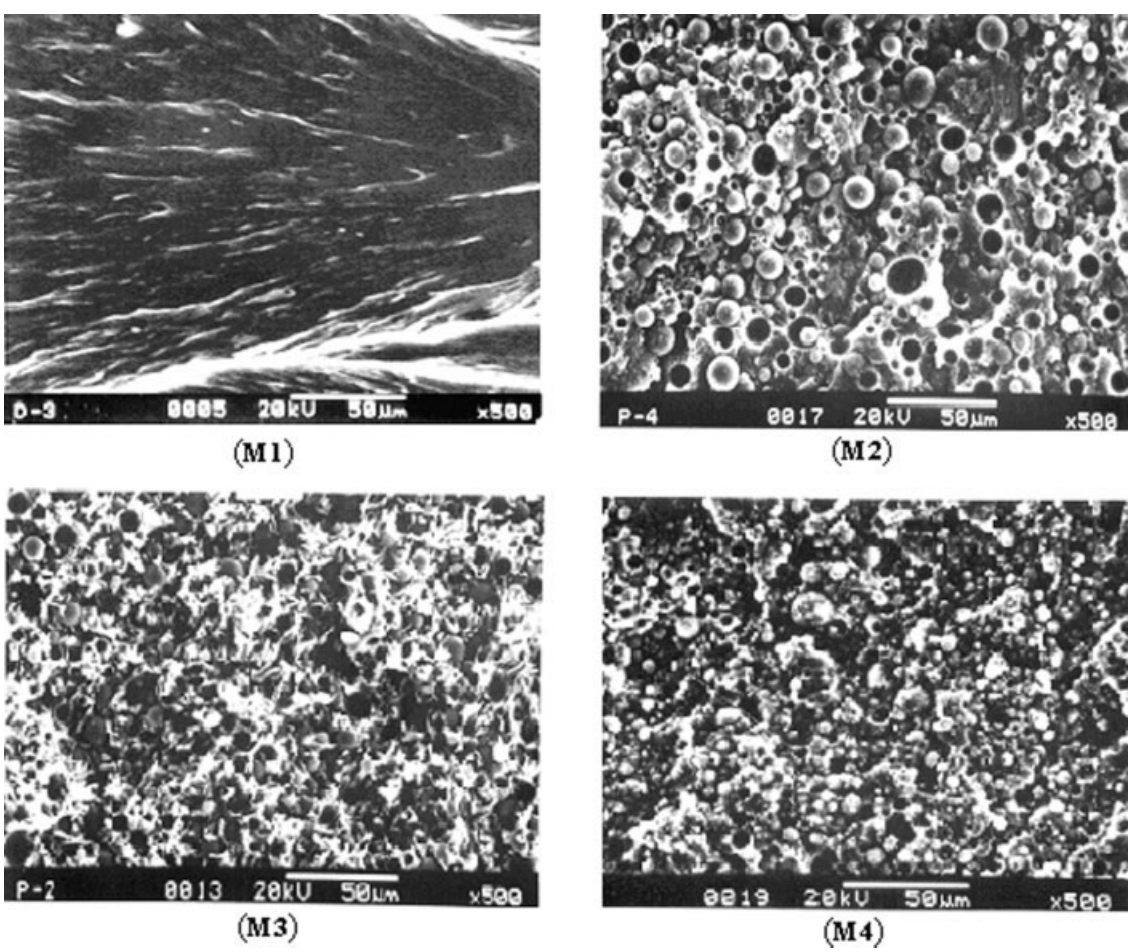

Figure 8 SEM photographs of fractured surfaces. (M1) PPS, (M2) binary blend, (M3) 2% MA-PP-added ternary blend, and (M4) 5% MA-PP-added ternary blend.

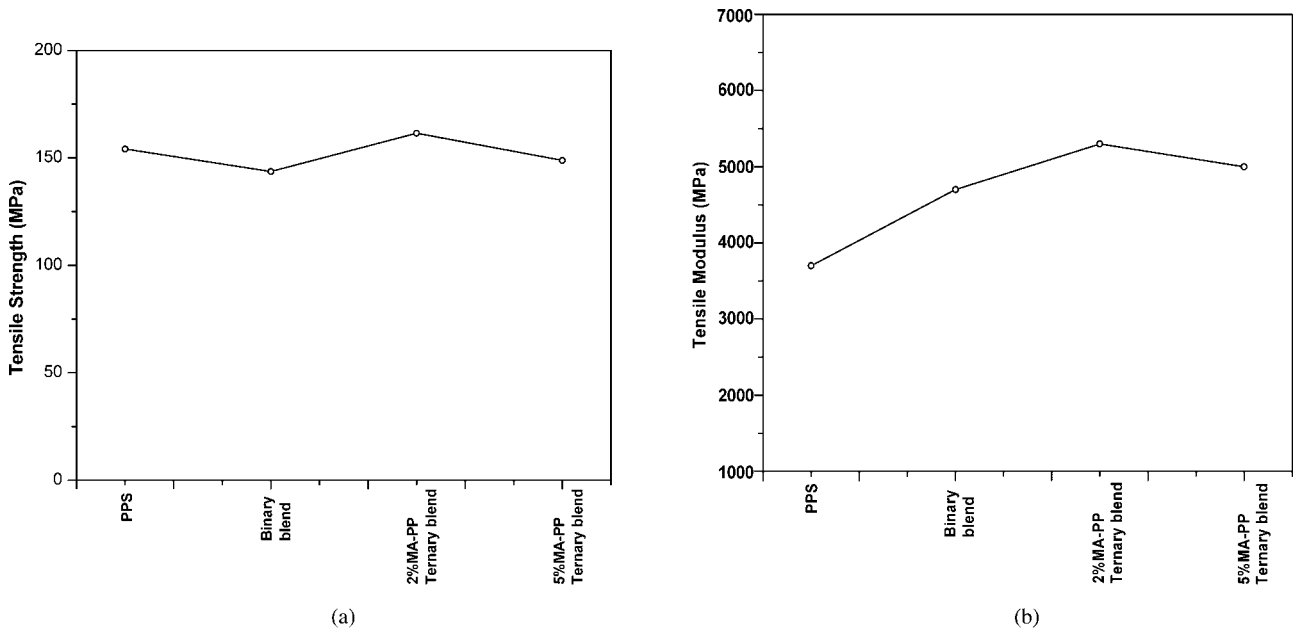

Figure 9 Mechanical properties of PPS and blends. (a) tensile strength and (b) tensile modulus. The inset shows the maximum when 2% MA-PP was added.

of mixture, which is the typical sign of an immiscible system. The tensile strength of the PPS-rich phase decreases with TLCP content because of the loss of ductility and failure at the interface, whereas the tensile modulus of the TLCP-rich phase increases because of the molecular orientation and the high modulus of TLCP phase. But in case of ternary blend systems, the tensile strength and modulus show interesting behaviors that depend on the amount of MA-PP added, i.e., they show maximum values when 2 wt % of MA-PP is added and then decrease when more MA-PP is added. A compatibilized composite has a larger frictional shear force due to the strong adhesion at the interface between the matrix and the fiber, thus requiring more energy to pull out the fibers.[22] As a result, the tensile strength of the system increases. If the fiber still maintains contact with the sheath of the matrix surrounding it, work must be done in pulling the fiber fragments against the restraining frictional force at the fiber matrix interface.[22] If the fiber does not maintain contact with the sheath of the matrix, the fibers can be easily pulled-out, so that elongation cannot be increased. However, additional energy must be expanded to break the strong adhesion at the interface in a compatibilized system. Fibers will not be simply debonded: they will sustain their fibril shapes over the gap between crack surfaces until additional energy is supplied.[22] This allows the blends containing a small amount of MA-PP to attain a greater strength and modulus than the binary system. Excess amount of compatibilizer, however, brings about the coalescence of dispersed phase. Owing to poor dispersion, the tensile strength and the modulus are decreased because both total contacting area and the energy restraining the crack area are decreased.

CONCLUSIONS

In situ composites of PPS/LCP/MA-PP were prepared. The addition of MA-PP as a compatibilizer results in a dramatic reduction of the dispersed LCP size. The miscibility between MA-PP and PPS or Vectra-A was determined by measuring the T_g shift by DSC and DMTA. The crystallization temperature of LCP shifts to the lower temperature side when blended with MA-PP. Addition of compatibilizer to PPS/LCP blends results in decreased viscosity. Morphological evidence demonstrated that addition of the correct amount of MA-PP reduces the LCP particle size and induces a fine distribution. However, optimum amounts of compatibilizer for the best mechanical properties and dispersion of LCP phase were observed. Excess amounts of MA-PP coalesce the LCP particle. The effectiveness of the compatibilizer depended on the absolute content of the compatibilizer. The mechanical properties (tensile strength as well as modulus) were improved when the proper amount of MA-PP is added, which enables improved adhesion at the interface.

References

1. Kiss, G. Polym Eng Sci 1987, 27, 410.
2. Pawlikowski, G. T.; Dutta, D.; Weiss, R. A. Ann Rev Mater Sci 1991, 21, 159.

3. Baird, D. G.; Wilkes, G. L. Polym Eng Sci 1983, 23, 632.
4. Crevecoeur, G.; Groeninckx, Polym Eng Sci 1990, 30, 532.
5. Williams, D. J. Adv Polym Tech 1990, 10, 173.
6. Xu, Q. W.; Leng, Y.; Mal, Y.-W. Polym Eng Sci 1996, 36, 769.
7. Dutta, D.; Fruitwala, H.; Kholi, A.; Weiss, R. A. Polym Eng Sci 1990, 30, 1005.
8. Ramanathan, R.; Blizard, K.; Baird, D. SPE ANTEC 1988, 46, 1123.
9. Heino, M. T.; Seppala, J. V. J Appl Polym Sci 1992, 44, 2185.
10. Seppala, J.; Heino, M.; Kapanen, C. J Appl Polym Sci 1992, 44, 1051.
11. Tsebrenko, M. V.; Danilova, G. P. J Non-Newtonian Fluid Mech 1989, 34, 26.
12. Shin, B. Y.; Chung, I. J. Polym J 1990, 30, 13.
13. Joslin, S.; Jackson, W.; Farris, R. J Appl Polym Sci 1994, 54, 439.
14. Kim, B. C.; et al. Polym Eng Sci 1996, 36, 574.
15. Seo, Y.; Hong, S. M.; Hwuang, S. S.; Park, T. S. Kim, K. U. Polymer 1995, 36, 515.
16. Holsti-Meittinen, R. M.; Heino, M. T.; Seppala, J. V. J Appl Polym Sci 1995, 57, 537.
17. Rabiej, S.; Ostrowska-Gumkowska, B.; Wlochowicz, A. Eur Polym J 1997, 33, 1031.
18. Wunderlich, B. Macromolecular Physics, Vol. 1; Academic Press: New York, 1973.
19. Klein, N.; Selivansky, D.; Maron, G. Polym Compos 1995, 16, 189.
20. Seo, Y.; Hong, S. M.; Kim, K. U. Macromolecules 1997, 30, 2978.
21. Shih, C. K. Polym Eng Sci 1976, 16, 328.
22. Seo, Y.; Hong, S. M.; Hwang, S. S. Park, T. S.; Kim, K. U.; Lee, S.; Lee, J. W. Polymer 1995, 36, 525.